Received 4 December 2025
Revised 15 January 2026
Accepted 9 February 2026

The probabilistic on and off fault displacement hazard analysis for high-speed railways crossing the middle Xiaojiang fault zone

Jiahui Feng
Railway Science and Technology Research and Development Center, China Academy of Railway Sciences Corporation Limited, Beijing, China

Abstract

Purpose – The rapid expansion of high-speed railway (HSR) networks in Western China has increased the exposure of linear infrastructure to active faults. This study establishes and applies a probabilistic fault displacement hazard analysis (PFDHA) framework to quantify both on-fault surface rupture and distributed off-fault permanent ground deformation (PGD) hazards for HSR crossings of the Xiaojiang Fault Zone (XJFZ).

Design/methodology/approach – A PFDHA framework is developed, integrating a Poissonian seismicity model with spatial rupture randomness. The methodology is applied to the XJFZ, which crosses the Nanning-Kunming (NK) and Shanghai-Kunming (SK) HSR. Permanent displacement hazards are evaluated for 2 probability levels: 10% and 2% probability of exceedance in 50 years.

Findings – Through the evaluation of displacement hazards for 50-year exceedance probabilities of 10% and 2%, this study finds that for the NK and SK HSR, permanent displacements at a 10% probability of exceedance range from 1.0 m to 2.9 m, peaking at fault intersections. Comparative analysis shows that traditional deterministic estimates (1.3–2.0 m) generally align with the probabilistic results but fail to capture the full range of risk.

Originality/value – This work adapts PFDHA to linear infrastructure in a tectonically active region of China, explicitly considering both on- and off-fault displacement within engineering-relevant corridors. The integration of regional rupture scaling and segment-based constraints provides a reproducible basis for displacement hazard assessment in HSR planning and retrofit.

Keywords High-speed railway (HSR), Probabilistic fault displacement hazard analysis (PFDHA), Xiaojiang fault zone (XJFZ), Permanent ground deformation (PGD), Seismic risk assessment

Paper type Technical paper

1. Introduction

A fundamental principle in critical infrastructure planning is the avoidance of active faults (Xu *et al.*, 2016). However, for trans-regional linear infrastructure projects–such as the Sichuan-Tibet Railway, the west-east gas transmission and the Shanghai-Kunming High-Speed Railway (SK HSR)–crossing active tectonic zones is often unavoidable due to topographic and routing constraints. The seismic vulnerability of these linear structures differs fundamentally from discrete buildings. While the primary threat to buildings is the inertial force generated by ground acceleration (shaking), the integrity of railways–particularly tunnels and bridges–is disproportionately threatened by permanent ground deformation (PGD). Surface fault rupture, the most severe form of PGD, involves the relative shearing of the ground surface along a fault trace. This displacement is often discrete, large in magnitude, and occurs instantaneously

Funding: This research is supported by the R&D Fund Project of China Academy of Railway Science Corporation Limited (No: 2024YJ120) and Sichuan Provincial Major Scientific and Technological Special Project (No: 2023ZDZX0030).

during a seismic event, imposing kinematic demands that far exceed the elastic capacity of conventional concrete linings or bridge bearings.

Post-earthquake field investigations, such as those following the 2022 Ms6.9 Menyuan earthquake, reveal that permanent surface displacement often causes more catastrophic damage to tunnels, bridges, and track systems than transient ground shaking (Zhang, Yuan, Zhou, & Fan, 2023; Chen, Geng, Chen, & Gu, 2023). The earthquake produced a surface rupture that directly intersected the Daliang Tunnel of the Lanzhou-Xinjiang High-Speed Railway (Yan, 2023). Additionally, studies on the Hualai section of the Beijing-Zhangjiakou High-Speed Railway indicate that fault slip significantly affects ground subsidence, with vertical displacements of 50 m below the surface entirely attributed to fault slip. Consequently, accurate quantification of fault displacement hazard is critical for the structural integrity and operational safety of these lifelines.

Currently, railway seismic design predominantly relies on deterministic seismic hazard analysis (DSHA). This approach typically estimates a “Maximum Credible Earthquake” (MCE) and assumes a uniform maximum displacement along the fault trace. For example, studies on the 2008 Wenchuan earthquake showed vertical displacements of 3–4 m, peaking at 6.5 m (Shen *et al.*, 2009). While DSHA provides a single design value, it fails to account for critical uncertainties in magnitude recurrence, rupture length, and the spatial distribution of slip. This limitation may result in either overly conservative designs or insufficient consideration of low-probability high-consequence events (Sun, 2002).

In contrast, probabilistic fault displacement hazard analysis (PFDHA) extends the probabilistic seismic hazard analysis (PSHA) framework to permanent ground deformation (PGD) and explicitly propagates both aleatory and epistemic uncertainties (Youngs *et al.*, 2003; Petersen *et al.*, 2011). Youngs *et al.* (2003) established the core formulation and a displacement model mainly for normal-fault events, whereas Petersen *et al.* (2011) further extended the framework to strike-slip faults and incorporated fault-trace location uncertainty, providing a practical basis for facility-scale applications. Subsequent studies in China applied PFDHA-type concepts to specific faults or developed local displacement models (e.g. Zhao, Liu, Shi, & Wu, 2008; Liu, Zhao, & Zhou, 2010; Jing, 2019). However, many applications still rely on global rupture-scaling relationships and the treatment of distributed (off-fault) deformation is often simplified, which is particularly important for long linear infrastructure. Meanwhile, regional studies have derived rupture-scaling relations for Mainland China (Cheng, Rong, Magistrale, Chen, & Xu, 2020) and proposed detailed segmentation and multi-segment rupture models for the Xiaojiang Fault Zone (XJFZ) (Cheng, Xu, Ren, Zhang, & Wu, 2021; Cheng, Xu, Ma, Xu, & Zhu, 2023), offering improved constraints on rupture dimensions and segment-based maximum magnitude. Nevertheless, an integrated on and off fault displacement hazard assessment for high-speed railways crossing the XJFZ remains limited. It should be emphasized that deterministic and probabilistic approaches are complementary: DSHA provides scenario-based bounding checks, whereas PFDHA yields hazard curves that support performance-based design and risk-informed decision-making for long linear corridors.

Despite its inclusion in guidelines by the international atomic energy agency (IAEA) (Valentini *et al.*, 2021), its application in the railway engineering sector remains limited. This study addresses this gap by applying a rigorous PFDHA framework to the XJFZ, a highly active system crossing the Nanning-Kunming (NK) and SK HSR. We aim to: (1) construct a probabilistic model tailored for linear infrastructure; (2) quantify the displacement hazard for varying return periods; and (3) compare these results with traditional deterministic methods to validate the model’s applicability for engineering design.

2. Probabilistic fault displacement hazard analysis (PFDHA)

2.1 Analytical framework

The PFDHA framework adopted in this study extends the standard PSHA formulation (Cornell, 1968) to evaluate PGD. Unlike PSHA, which predicts ground motion intensity, PFDHA integrates the probability of surface rupture occurrence and the conditional probability distribution of displacement amplitude (Petersen *et al.*, 2011; Youngs *et al.*, 2003). The annual rate λ of displacement D exceeding a threshold d at a specific site (x, y) is calculated as the Equation (1):

$$p\,(D \geq d) \approx \lambda\,(D \geq d) = \exp\left(\sum_{i=1}^{k} v_i \int_{M_0}^{M_{uz}} \int_{r} f_i(m) f_i(r|m)\, P\,(slip|m,r)\, P\,(D \geq d|m,r,slip)\, drdm\right) \tag{1}$$

Where $p\,(D \geq d)$ is the probability that the permanent displacement D at an engineering site is not less than a given value d; v_i is the annual rate of earthquakes for source i with magnitude m; $f_i\,(m)$ is the probability density function (PDF) of the magnitude where an earthquake on source i between M_0 and the maximum magnitude M_{uz}; $f_i\,(r|m)$ is the conditional PDF of the distance r from the site to the rupture, accounting for the randomness of the rupture location on the fault plane.

$P\,(slip|m,r)$ represents the probability that a rupture of magnitude m at distance r extends to the ground surface. Deep-seated events or smaller magnitude events may terminate before reaching the ground. Furthermore, even if the fault ruptures the surface, the rupture trace has finite length $L\,(m)$ and finite width $W\,(m)$. The site only experiences displacement if it falls within the geometric footprint of the rupture. For each magnitude, the rupture surface is assumed to float on the fault plane, and the number of rupture surfaces that extend to the surface is counted. Specifically, if there are N possible rupture surfaces for a given magnitude, and n of them extend to the surface, then $P\,(slip|m,r) = \mathrm{n}/N$ (Figure 1).

$P\,(D \geq d|m,r,slip)$ is the conditional probability that surface displacement exceeds d, given that surface rupture occurs. Displacement is not uniform; it is typically modeled as an elliptical or bell-shaped distribution peaking at the center of the rupture. Additionally, for any given point, there is natural variability.

In practical calculations, Equation (1) is typically replaced by a discrete form to substitute for integral operations. Three types of rupture may occur on the fault surface: the first type occurs at a deeper location, where the rupture does not extend to the surface and does not cause permanent displacement at the target point (x_0, y_0), as shown in Figure 2, the first rupture zone. The second type extends to the surface but does not reach the target point, as shown in Figure 2, the second rupture zone. The third type extends to the surface and also reaches the target point, as shown in Figure 2, the third rupture zone. Only this type of rupture contributes to the permanent displacement at the target point.

For reproducibility, the computational steps are summarized as follows: (1) Define fault source geometry and discretize the surface traces at 1 km spacing; (2) Discretize the magnitude range $[M_{min}, M_{max}]$ with ΔM and compute annual occurrence rates for each bin using the truncated Gutenberg-Richter model; (3) For each magnitude bin, estimate rupture dimensions using the selected scaling relations and generate floating rupture realizations along strike; (4) Evaluate $P\,(slip|m,r)$ as the fraction of surface-breaking ruptures that intersect the site; (5) Compute the conditional displacement exceedance probability $P\,(D \geq d|m,r,slip)$ using the adopted along-strike slip distribution and off-fault attenuation with lognormal variability (truncated at $\pm$ 3σ); (6) Integrate over magnitude and rupture location to obtain the annual exceedance rate λ (D $\geq$ d); (7) Convert $\lambda\,(D \geq d)$ to time-dependent exceedance probability for a given design life T using P = 1-exp $[-\lambda\,(D \geq d)\,T]$.

2.2 Source characterization and scaling relationships

The implementation of PFDHA requires rigorous characterization of seismic sources and fault geometry. The model inputs are categorized as follows:

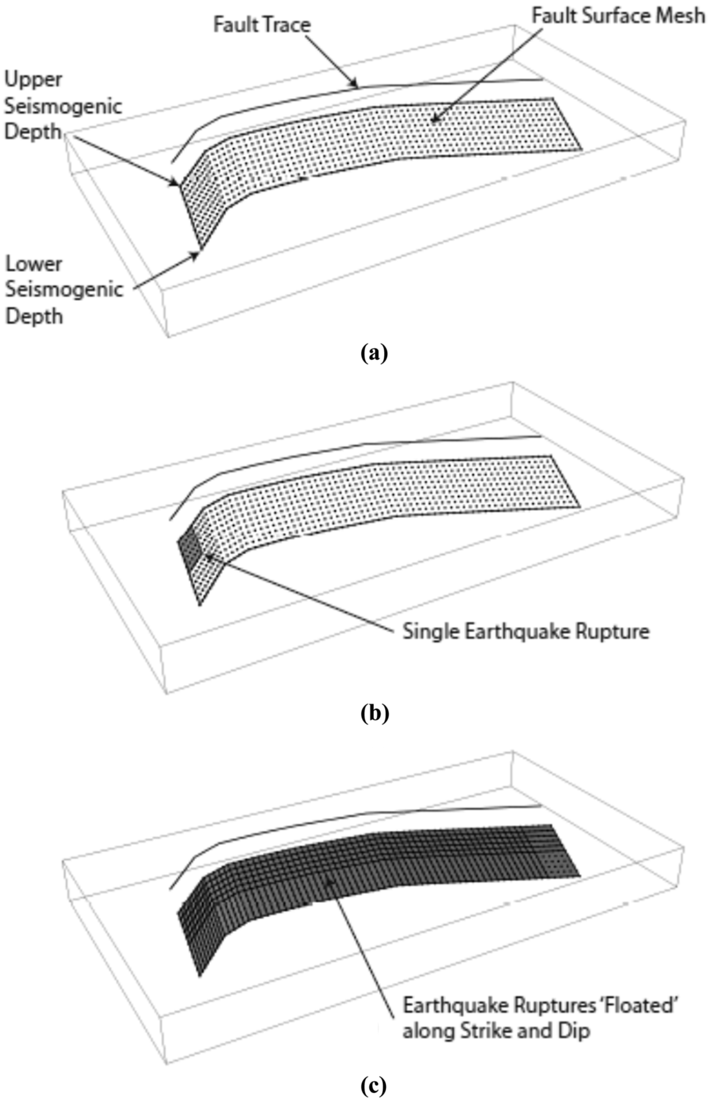

Figure 1. Fault-surface construction and rupture-area floating schematic (a) The fault surface is created by projecting the fault trace from the Earth's surface to the lower seismogenic depth at a dip angle and then discretised into a mesh; (b) An earthquake rupture is defined as a portion of this meshed fault surface; (c) All possible rupture locations are simulated by allowing the rupture patch to "float" both along strike and along dip. Source(s): Edited from Pagani *et al.* (2014)

2.2.1 Seismicity model. Earthquake recurrence is modeled using a truncated Gutenberg-Richter relationship, defined by the *a*-value (activity rate), *b*-value (relative magnitude distribution), and maximum magnitude M_{uz}. Background seismicity is assumed to follow a Poisson process. The probability of an earthquake of magnitude M occurring is given by Equation (2):

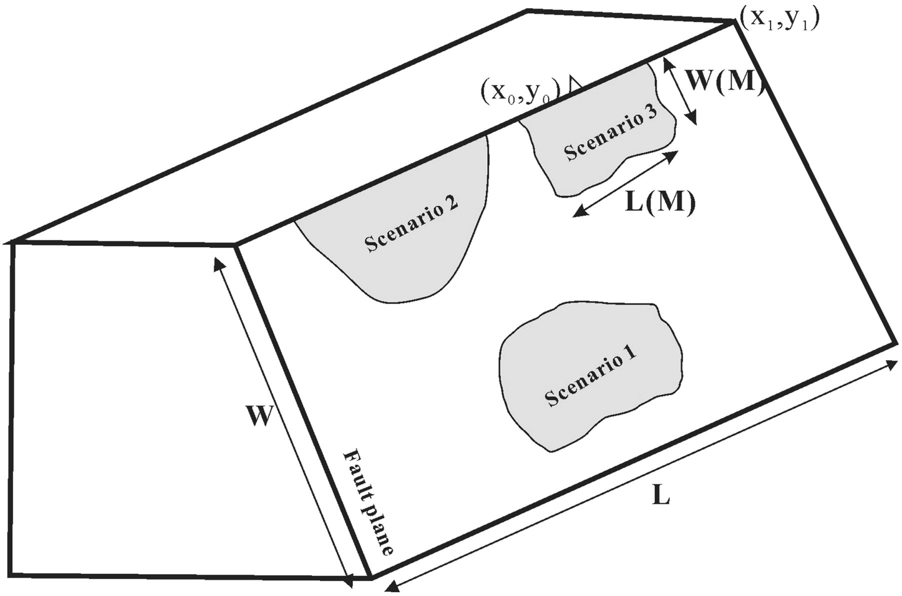

Figure 2. The relationship between fault rupture and surface displacement on the fault surface. Source(s): Author's own work

$$P(M) = \frac{\beta \exp(-\beta(M - M_{\min}))}{1 - \exp(-\beta(M_{uz} - M_{\min}))} \tag{2}$$

where $\beta = b ln 10$.

2.2.2 Geometric and rupture parameters. Fault sources are modeled as 3D planes defined by strike, dip, and depth. To account for aleatory uncertainty in rupture dimensions, we employ empirical scaling relationships. Rupture length and width are primarily estimated using the regional rupture-scaling relations for Mainland China proposed by Cheng *et al.* (2020), while the global regressions of Wells and Coppersmith (1994) are retained as an alternative branch to capture epistemic uncertainty. The probability of slip at a specific site, $P(slip)$, is determined by the geometric relationship between the potential rupture trace and the site coordinates. The displacement variability is modeled as Equation (3):

$$\ln(D) = \mu(m) + \epsilon\sigma \tag{3}$$

where $\mu(m)$ is the mean log-displacement derived from global or regional regressions, ϵ is the aleatory standard deviation, and σ is the number of standard deviations. In our implementation, the probability distribution is truncated at 3 standard deviations to exclude physically unrealistic displacement values.

2.2.3 Displacement attenuation. The conditional probability of displacement $P(D \geq d)$ accounts for the variability in displacement along the rupture strike. We adopt an elliptical distribution model where displacement peaks at the rupture center and tapers towards the ends, incorporating a log-normal standard deviation to capture observational scatter (Petersen *et al.*, 2011).

3. Case study: the XJFZ railway crossing

3.1 Seismotectonic setting

The study area focuses on the XJFZ, a highly active left-lateral strike-slip system defining the southeastern boundary of the Sichuan-Yunnan Block. It is a highly active left-lateral strike-slip system extending approximately 400 km north-to-south. Geometrically, the fault is complex. While the northern segment (from Qiaojia to Dongchuan) appears as a single main trace, the central segment (from Dongchuan to Fuxian Lake)–which is the focus of this study–bifurcates into 2 distinct strands: the Eastern Branch and the Western Branch. These 2 branches run parallel with a separation distance of 12–16 km, forming an "en échelon" pattern that creates local pull-apart basins, such as the Songming and Yanglin basins (Chang, Chen, Li, & Zhou, 2021). Recent fault-system studies further suggest that the middle XJFZ can be described by a segmented structure with potential multi-segment ruptures, which provides additional constraints for source parameterization (Cheng *et al.*, 2021, 2023).

The observed left-lateral slip rate is approximately 10 mm/year for the overall system. Specifically, the Western Branch exhibits a higher slip rate of 7–9 mm/year, while the Eastern Branch moves at 5–7 mm/year (Wang & Shen, 2020; Yi, Wen, & Su, 2008). The XJFZ has a well-documented history of large-magnitude earthquakes. Historical chronicles and paleoseismic trenches indicate that the fault has hosted at least 17 earthquakes with magnitudes greater than 6.0 in the past 500 years (Tan, Liang, & Ma, 2023). Notable events include the 1,500 Yiliang M 7.0 earthquake and the 1833 Songming M 8.0 earthquake. The 1833 Songming event is particularly significant for this hazard analysis. With an estimated rupture length exceeding 100 km and peak displacements likely surpassing 6 m, it represents the characteristic "maximum earthquake" for the region. The recurrence interval for $M \geq 7.0$ events is estimated to be approximately 110 years, with the last major rupture occurring nearly two centuries ago, suggesting a high potential for future large-scale events (Zhao *et al.*, 2015).

The SK and NK HSR are vital arteries in China's "Eight Vertical and Eight Horizontal" railway network. The Kunming-Qujing section of SK HSR and the Mile-Kunming section of NK HSR are geographically forced to cross the XJFZ. According to the "Fifth Generation Seismic Ground Motion Parameter Zonation Map of China", the region is classified as a high-intensity zone, with Peak Ground Accelerations (PGA) reaching 0.4 g. However, as noted in the introduction, the PGA maps do not quantify the discrete displacement hazard at the fault crossing points. The railway alignment intersects the fault branches at near-perpendicular or oblique angles. We analyze 3 intersection nodes per railway (H1-H3, N1-N3) where active traces cross track alignments at 30–45° angles.

3.2 Model inputs and parameters

To implement the PFDHA for the SK and NK HSR crossings, the following parameters were established (Table 1):

(1) *Fault geometry:* The fault traces were discretized at 1 km intervals. The fault plane is assumed to be near-vertical (strike-slip), extending to a seismogenic depth of 20 km. The western and eastern branches are assigned slip-rate ranges of 7–9 mm/yr and 5–7 mm/yr, respectively (Yi *et al.*, 2008; Wang & Shen, 2020), which are consistent with the ranges reported by Cheng *et al.* (2021) for the Xiaojiang fault branches.

(2) *Magnitude limits:* Based on the historical catalog and segmentation models, the maximum magnitude (M_{max}) was set to 8.0. The minimum threshold (M_{min}) for surface displacement calculation was set to 7.0. The magnitude bins are discretized with an interval of 0.1, consistent with standard earthquake hazard calculations.

(3) *Recurrence parameters:* A truncated Gutenberg-Richter recurrence model is applied. Based on the regional earthquake catalog and the "Fifth Generation Seismic Ground Motion Parameter Zonation Map of China", we adopted an a-value of 3.63 and a b-value of 0.72.

Table 1. List of parameters required for calculation

Model component/ parameter	Value/implementation in this study
Fault dip	90° (near-vertical)
Seismogenic depth	20 km
Trace discretization	1 km
Magnitude	$M_{min} = 7.0$, $M_{max} = 8.0$, $\Delta M = 0.1$
Gutenberg-Richter	a = 3.63, b = 0.72 (truncated)
Slip rate	West branch: 7–9 mm/yr East branch: 5–7 mm/yr
Scaling	$log\,10(RLD) = -2.67 + 0.63Mw$ (Cheng *et al.*, 2020) $log\,(MD) = -7.03 + 1.03M$ (Wells & Coppersmith, 1994)
Off-fault attenuation	Fault-normal attenuation within 100 m S (x) = S (A)·(1 − x/100 m) for 0 ≤ x ≤ 100 m S (x) = 0 beyond 100 m
Variability	lognormal, truncated at ± 3σ

Source(s): Author's own work

(4) *Scaling relations:* Rupture dimensions (RLD/SRL and RW) are primarily estimated using the Mainland-China scaling relations of Cheng *et al.* (2020) (Equation (4)). For large strike-slip earthquakes, RW is assumed to saturate near the seismogenic thickness (~20–21 km). The maximum surface displacement (MD, in meters) at the rupture center is estimated using the strike-slip displacement–magnitude regression of Wells and Coppersmith (1994), and the associated aleatory variability is represented by a lognormal distribution truncated at ± 3σ (Equation (5)).

$$\log 10\,(\mathrm{RLD}) = -2.67 + 0.63\,\mathrm{Mw} \tag{4}$$

$$\mathrm{Log}\,(\mathrm{MD}) = -7.03 + 1.03\mathrm{M} \tag{5}$$

(5) *Displacement attenuation:* A linear attenuation model is assumed from the center of the rupture to the ends of the fault trace. Along the fault-normal direction the displacement decays linearly from the fault plane to the 100-m offset according to S (x) = S (A)·(1–x/100 m), 0 ≤ x ≤ 100 m, while along-strike the displacement at a point A located a distance AC from the fault center C is given by d· AC/(L/2), where d is the maximum displacement at C and L is the total fault length.

(6) *Target sites:* Displacement hazard was calculated for 84 points along the SK HSR (Kunming segment) and 38 points along the NK HSR, covering a corridor of 25 km on either side of the fault trace.

(7) *Annual and time-dependent exceedance probability:* The annual exceedance probability (P (Y > y)) and the time-dependent exceedance probability (P (>y)) are related through Equations (6) and (7). The annual exceedance probability can be converted to a time-dependent probability (e.g. 50 or 100 years), and interpolation is used to determine the parameters for specified probability levels (e.g. 2%, 10%, 53%).

$$P_1(Y > y) = 1 - [1 - P_t(Y > y)]^{1/t} \tag{6}$$

$$P_t(Y > y) = 1 - [1 - P_1(Y > y)]^t \tag{7}$$

4. Results

The probabilistic hazard was evaluated for 2 standard engineering performance levels: 10% probability of exceedance in 50 years (Design Basis Earthquake), and 2% probability of exceedance in 50 years (Maximum Considered Earthquake).

For the SK HSR (Qujing to Kunming segment), the permanent displacement at a 10% exceedance probability in 50 years ranges from 1.02 m to 2.86 m. The hazard is non-uniform, peaking at the specific intersection points with the fault branches (Points H1-H3), where displacements reach 2.84 m, 2.81 m, 2.70 m; under the rarer 2% exceedance probability scenario, displacements increase marginally to 2.88 m, 2.84 m, 2.74 m at these intersections. This localization confirms the model's physical fidelity: hazard is highest where the railway sits directly atop the fault trace and decays rapidly as the distance from the fault increases. The relatively small difference between the 10% and 2% values suggests that for this highly active fault, the "characteristic" large earthquake dominates the hazard at both return periods. Once the threshold for a major event is crossed, the displacement is substantial; there are few "small" rupture scenarios contributing to the hazard at the exact crossing point.

Similarly, for the NK HSR (Mile to Kunming segment), the 10% exceedance displacement ranges from 1.00 m to 1.99 m, with intersection points (N1-N3) exhibiting values between 1.48 m, 1.97 m, 1.42m; under the rarer 2% exceedance probability scenario, displacements increase marginally to 1.48 m, 2.07 m, 1.44 m at these intersections. The hazard probability drops sharply for displacements exceeding 2 m, as shown in the annual exceedance probability curves (Figure 3).

The annual exceedance probability curves (Figure 4) reveal a distinct hazard gradient. For displacement values up to 1.0 m, the probability of exceedance remains high and relatively

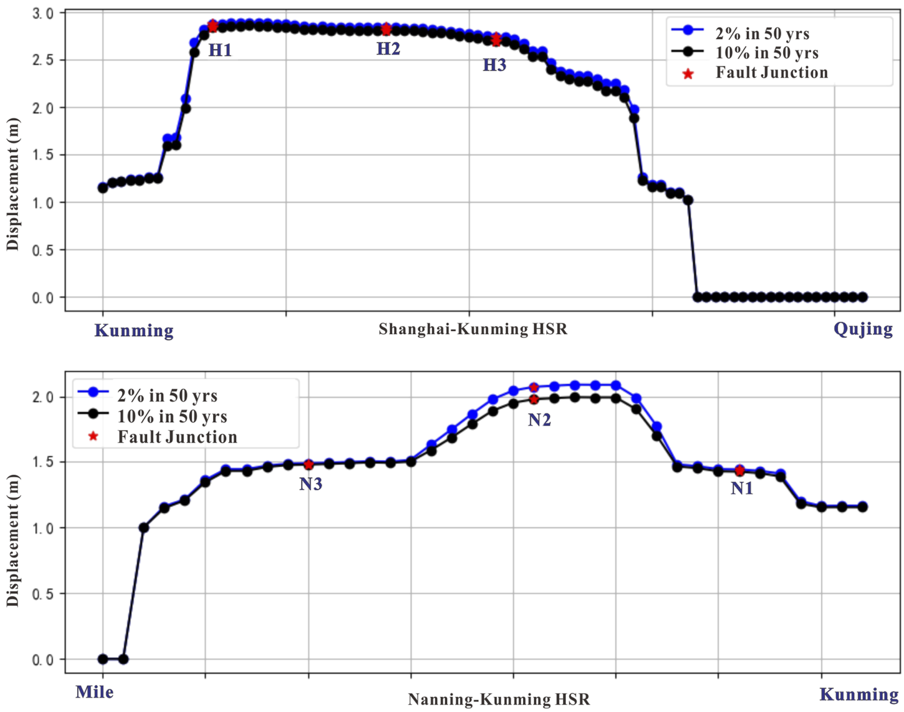

Figure 3. Fault displacement with 2% and 10% probabilities of exceedance in 50 years along the SK and NK HSR. Source(s): Author's own work

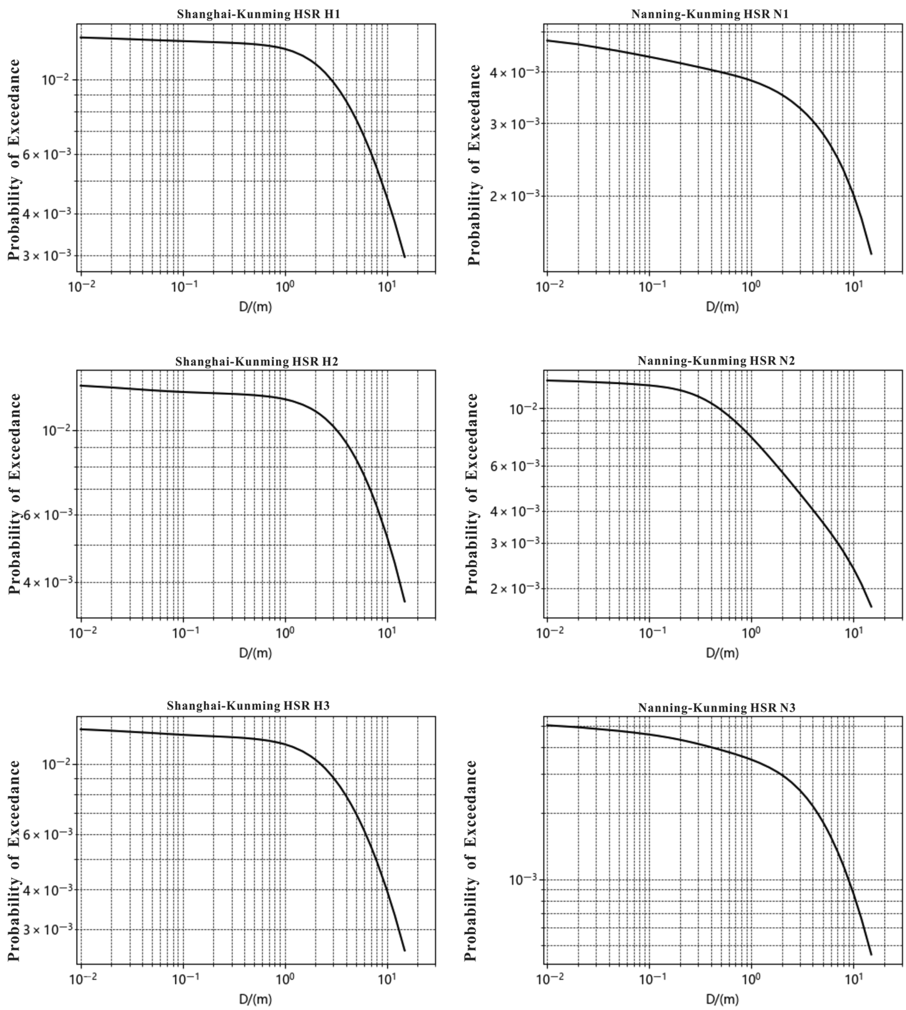

Figure 4. Annual probability of exceedance for permanent displacement at fault-crossing sites of the SK and NK HSR. Source(s): Author's own work

constant. However, for displacements exceeding 1.0 m, the probability drops sharply. The probability of exceeding 10 m of displacement is negligible (<0.3% annual probability), framing the realistic bounds for engineering design.

5. Discussion

To validate the PFDHA results, we compared them with standard deterministic estimates derived from paleoseismological data. Excavations along the Xiaojiang Fault reveal a recurrence interval of approximately 2000–2,500 years for the eastern branch and 370–440 years for the western branch (Chang *et al.*, 2021; Tan *et al.*, 2023). Using the empirical slip-rate method and characteristic earthquake models (Zhang *et al.*, 2003; Deng, Gao, & Yang, 2009), the deterministic maximum displacement for a 100-year design life is estimated at *1.3–2.0 m* (left-lateral strike-slip).

Our PFDHA results for the 475-year return period (10% in 50 years) corresponds to displacements of 1.02–2.89 m at the fault crossings. This indicates that the PFDHA model provides a robust and slightly conservative safety margin, appropriately capturing the aleatory uncertainty associated with extreme events like the 1833 Songming earthquake. The deterministic method often relies on the "mean" or "observed" values from trenches. However, trenches might miss the point of maximum slip along a rupture. This comparison confirms that the PFDHA results are physically reasonable and suitable for guiding engineering design.

While the values align, the PFDHA method offers distinct advantages over the single-value deterministic approach. PFDHA provides a continuous hazard curve, allowing engineers to assess risks for different performance objectives (e.g. "serviceability" at frequent events vs. "life safety" at rare events). The deterministic method might mandate a 2.0 m displacement design regardless of probability. PFDHA provides a continuous hazard curve so that design actions can be explicitly linked to performance objectives by applying PFDHA and target reliabilities. For example, it shows that although 2.0 m is plausible at the crossing, displacements exceeding 3.0 m have very low probability, enabling engineers to prioritize robustness and mitigation where it is most needed while avoiding unnecessary conservatism.

From a methodological perspective, DSHA and PFDHA serve complementary purposes. DSHA is scenario-driven and is effective for defining credible upper-bound checks (e.g. MCE-based displacement demands) when the design target is an ultimate limit state. However, DSHA does not provide exceedance probabilities and thus cannot directly support multiple performance objectives (e.g. serviceability versus life-safety) along long corridors. In contrast, PFDHA integrates rupture occurrence rates, rupture-location uncertainty, and conditional displacement variability to provide hazard curves, enabling risk-informed prioritization of mitigation at the most hazardous crossings.

Several limitations should be acknowledged. First, due to limited near-fault observations for the Xiaojiang system, the off-fault displacement attenuation is simplified as a linear decay to zero at 100 m; distributed deformation beyond this distance may not be fully captured. Second, although regional rupture-scaling relations and segmentation insights are incorporated, epistemic uncertainty remains for multi-segment ruptures and for the spatial distribution of slip. Third, earthquake occurrence is modeled as a stationary Poisson process; where recurrence intervals are well constrained, time-dependent renewal models could be explored.

Future work should focus on (1) collecting additional paleoseismic, InSAR, and GNSS constraints to calibrate off-fault deformation width and to refine fault-trace location uncertainty; (2) incorporating fault-system multi-segment rupture models and stress interactions; and (3) coupling PFDHA with physics-based dynamic rupture simulations and targeted geophysical surveys (e.g. shallow seismic imaging, resistivity and microtremor arrays) to better constrain fault geometry and near-surface structure, thereby improving displacement prediction for railway design.

6. Conclusions

This study presented a probabilistic on and off fault displacement hazard analysis for HSR crossing the seismically active XJFZ. The key conclusions are:

High hazard identification: The probabilistic model identifies critical intersection points where 50-year permanent displacements at a 10% exceedance probability reach 1.02–2.86 m for the SK HSR and 1.0–1.99 m for the NK HSR.

Methodological validation: The probabilistic estimates align well with deterministic values derived from paleoseismic slip rates (1.3–2.0 m), validating the robustness of the PFDHA framework for this region.

Implications for practice: Unlike deterministic methods that provide a single "worst-case" scenario, PFDHA generates full hazard curves. This enables a performance-based design approach, allowing railway engineers to implement targeted mitigation measures–such as route adjustments or flexible track systems–commensurate with the specific risk level of each rail segment.

This research establishes a scientific basis for seismic design in western China's railway network and offers a replicable framework for assessing fault displacement hazards in other linear infrastructure projects globally.

References

Chang, Y. Q., Chen, L. C., Li, X., & Zhou, Q. Y. (2021). The late quaternary activity of the fault along the western margin of the Yiliang basin of the Xiaojiang fault zone. *Journal of Seismological Research*, *44*(2), 152–161, (in Chinese).

Chen, P., Geng, P., Chen, J., & Gu, W. (2023). The seismic damage mechanism of Daliang tunnel by fault dislocation during the 2022 Menyuan Ms6.9 earthquake based on unidirectional velocity pulse input. *Engineering Failure Analysis*, *145*, 107047. doi: 10.1016/j.engfailanal.2023.107047.

Cheng, J., Rong, Y. F., Magistrale, H., Chen, G. H., & Xu, X. (2020). Earthquake rupture scaling relations for mainland China. *Seismological Research Letters*, *91*(1), 248–261. doi: 10.1785/0220190129.

Cheng, J., Xu, X. W., Ren, J. J., Zhang, S. M., & Wu, X. Y. (2021). Probabilistic multi-segment rupture seismic hazard along the Xiaojiang fault zone, Southeastern Tibetan plateau. *Journal of Asian Earth Sciences*, *221*, 104940. doi: 10.1016/j.jseaes.2021.104940.

Cheng, J., Xu, C., Ma, J., Xu, X. W., & Zhu, P. (2023). From active fault segmentation to risks of earthquake hazards and property and life losses–a case study from the Xianshuihe-Xiaojiang fault zone. *Science China Earth Sciences*, *66*(6), 1345–1364. doi: 10.1007/s11430-022-1076-y.

Cornell, C. A. (1968). Engineering seismic risk analysis. *Bulletin of the Seismological Society of America*, *58*(5), 1583–1606. doi: 10.1785/bssa0580051583.

Deng, Q. D., Gao, X., & Yang, H. (2009). Fault block tectonics, active fault-block tectonics and earthquake activity. *Chinese Journal of Geology*, *44*(4), 1083–1093, (in Chinese).

Jing, X. (2019). Study on prediction model of surface permanent displacement of strike-slip faults. *World Earthquake Engineering*, 2, 18–23, (in Chinese).

Liu, Y. Q., Zhao, J. S., & Zhou, Z. H. (2010). Evaluation on permanent peak displacement near causative faults. *Journal of Basic Science and Engineering*, *18*(S1), 217–224, (in Chinese).

Pagani, M., Monelli, D., Weatherill, G., Danciu, L., Crowley, H., Silva, V., . . . Vigano, D. (2014). OpenQuake engine: An open hazard (and risk) software for the global earthquake model. *Seismological Research Letters*, *85*(3), 692–702. doi: 10.1785/0220130087.

Petersen, M. D., Dawson, T. E., Chen, R., Cao, T., Wills, C. J., Schwartz, D. P., & Frankel, A. D. (2011). Fault displacement hazard for strike-slip faults. *Bulletin of the Seismological Society of America*, *101*(2), 805–825. doi: 10.1785/0120100035.

Shen, Z. K., Sun, J. B., Zhang, P. Z., Wan, Y. G., Wang, M., Bürgmann, R., . . . Wang, Q. L. (2009). Slip maxima at fault junctions and rupturing of barriers during the 2008 Wenchuan earthquake. *Nature Geoscience*, *2*(10), 718–724. doi: 10.1038/ngeo636.

Sun, J. B. (2002). A GlS-based system for probability evaluation of potential surface displacement on active fault segments associated with earthquakes-theory and practice. MA thesis, Beijing: Institute of Geology, China Earthquake Administration. (in Chinese).

Tan, X., Liang, K., & Ma, B. Q. (2023). A review of research progress on the late quaternary activities of the Xiaojiang Fault Zone. *Technology for Earthquake Disaster Prevention*, *18*(4), 757–772, (in Chinese).

Valentini, A., Fukushima, Y., Contri, P., Ono, M., Sakai, T., Thompson, S. C., . . . Youngs, R. R. (2021). Probabilistic Fault Displacement Hazard Assessment (PFDHA) for nuclear installations according to IAEA safety standards. *Bulletin of the Seismological Society of America*, *111*(5), 2661–2672. doi: 10.1785/0120210083.

Wang, M., & Shen, Z. K. (2020). Present-day crustal deformation of continental China derived from GPS and its tectonic implications. *Journal of Geophysical Research: Solid Earth*, *125*(2). doi: 10.1029/2019jb018774.

Wells, D. L., & Coppersmith, K. J. (1994). New empirical relationships among magnitude, rupture length, rupture width, rupture area, and surface displacement. *Bulletin of the Seismological Society of America*, *84*(4), 974–1002. doi: 10.1785/bssa0840040974.

Xu, X. W., Guo, T. T., Liu, S. Z., Yu, G. H., Chen, G. H., & Wu, X. Y. (2016). Discussion on issues associated with setback distance from active fault. *Seismology and Geology*, *38*(3), 456–468, (in Chinese).

Yan, Y. (2023). The tunnel damage effects and implications of the coseismic rupture of the Menyuan Ms 6.9 Earthquake in Qinghai, China. *Journal of Geomechanics*, *29*(6), 869–878, (in Chinese).

Yi, G. X., Wen, X. Z., & Su, Y. J. (2008). Study on the potential strong-earthquake risk for the eastern boundary of the Sichuan-Yunnan active faulted-block, China. *Chinese Journal of Geophysics*, *51* (6), 1719–1725, (in Chinese).

Youngs, R. R., Arabasz, W. J., Anderson, R. E., Ramelli, A. R., Ake, J. P., Slemmons, D. B., . . . Toro, G. R. (2003). A Methodology for probabilistic fault displacement hazard analysis (PFDHA). *Earthquake Spectra*, *19*(1), 191–219. doi: 10.1193/1.1542891.

Zhang, P. Z., Deng, Q. D., Zhang, G. M., Ma, J., Gan, W. J., Min, W., . . . Wang, Q. (2003). Active tectonic blocks and strong earthquakes in the continent of China. *Science China Earth Sciences*, *33*(Supplement 2), 13–24. doi: 10.1360/03dz0002, (in Chinese).

Zhang, Y. F., Yuan, K., Zhou, W. J., & Fan, J. W. (2023). Study on structural deformation characteristics and surface crack distribution of girder tunnel across Lenglongling fault caused by Menyuan earthquake. *Chinese Journal of Rock Mechanics and Engineering*, *42*(5), 1055–1069, (in Chinese).

Zhao, J. S., Liu, Y. Q., Shi, L. J., & Wu, J. F. (2008). A probabilistic approach to evaluate permanent displacement crossing fault by 4th generation seismic zoning map of China. *Earthquake Engineering and Engineering Dynamics*, *28*(4), 22–27, (in Chinese).

Zhao, J., Jiang, Z. S., Niu, A. F., Liu, J., Wu, Y., Wei, W., . . . Yan, W. (2015). Study on dynamic characteristics of fault locking and fault slip deficit in the eastern boundary of the Sichuan-Yunnan rhombic block. *Chinese Journal of Geophysics*, *58*(3), 872–885, (in Chinese).

Corresponding author
Jiahui Feng can be contacted at: fengjiahuifjh@126.com

Jiahui Feng is an Assistant Research Fellow at the Railway Engineering Research Institute, China Academy of Railway Sciences Corporation Limited. He received his Ph. D. from the Institute of Geology, China Earthquake Administration. His research focuses on seismotectonics, seismic hazard analysis, and earthquake early warning technology, with extensive experience in both technical development and product innovation. He has authored over 10 papers in authoritative journals, including 3 first-author publications in SCI Q2 and EI indexed journals, covering cutting-edge fields such as tectonophysics and earthquake early warning systems.